European Journal of Neuroscience, Vol. 6, pp. 1583–1588, 1994

Cortical Magnification Theory Fails to Predict Visual Recognition

Hans Strasburger, Ingo Rentschler and **Lewis O. Harvey, Jr**[1]
Institute for Medical Psychology, University of Munich, Goethestraβe 31, D-80336 Munich, Germany
[1]Department of Psychology, University of Colorado at Boulder, Boulder, CO 80309, USA

Key words: human, peripheral vision, contrast sensitivity, pathways, visual fields, models

Abstract

The sense of form is poor in indirect view. Yet the cortical magnification theory asserts that the disadvantage can be made up by scaling the image size according to the spatial variation in the mapping of the retina onto the cortex. It is thus assumed that all visual information passes through a functionally homogeneous neural circuitry, with the spatial sampling of input signals varying across the visual field. We challenge this notion by showing that character recognition in the visual field cannot be accommodated by any concept of sole size scaling but requires increasing both size and contrast of the target being viewed. This finding is formalized into a hyperbolic law which states that target size multiplied by log contrast is constant across the visual field. We conclude that the scalar cortical magnification theory fails for character recognition since the latter depends on multidimensional pattern representations in higher, i.e. striate and prestriate, cortical areas.

The tenet of cortical magnification theory is that properties of the primary pathway, from the retina to the cortex, are fully responsible for any behavioural changes that occur between central and peripheral vision. Opposing this are claims that more complex visual processing depends on the interaction of filter mechanisms (Rentschler and Treutwein, 1985; Bennett and Banks, 1987) or receptive field types (Livingstone and Hubel, 1985) having different scaling properties.

The functional consequences of retino-cortical mapping may be studied in two ways. In the direct approach spatial thresholds (e.g. grating resolution) are measured at various retinal loci (Weymouth, 1958; Daniel and Whitteridge, 1961; Cowey and Rolls, 1974; Koenderink *et al.*, 1978a) and the resulting function is compared with the geniculate and cortical mapping functions (Weymouth, 1958; Drasdo, 1977, 1989; Van Essen *et al.*, 1984; Perry and Cowey, 1985; Virsu *et al.*, 1987; Wässle *et al.*, 1989). In the indirect approach, the stimulus size is increased in order to compensate for the fall-off in performance found in indirect view (Weymouth, 1958; Daniel and Whitteridge, 1961; Cowey and Rolls, 1974; Drasdo, 1977, 1989; Koenderink *et al.*, 1978a, b; Rovamo *et al.*, 1978; Rovamo and Virsu, 1979; Virsu and Rovamo, 1979; Van Essen *et al.*, 1984; Perry and Cowey, 1985; Virsu *et al.*, 1987; Wässle *et al.*, 1989). When the increase in size is in inverse proportion to the cortical magnification M, it is called M-scaling.

M-scaling successfully equalizes performance for some visual functions, is controversial for others and clearly fails for a third group of functions. Functions which can be scaled successfully are two-point separation in the near periphery (Aubert and Foerster, 1857), grating acuity/minimal angle of resolution (Wertheim, 1894; Weymouth, 1958; Daniel and Whitteridge, 1961; Cowey and Rolls, 1974; Drasdo, 1977; Rovamo and Virsu, 1979), Snellen acuity (Ludvigh, 1941), diameter of Panum's fusion area (Ogle, 1950), migraine scotoma size (Drasdo, 1977), and grating contrast sensitivity as a function of both spatial frequency (Hilz and Cavonius, 1974; Koenderink *et al.*, 1978a; Rovamo *et al.*, 1978; Rovamo and Virsu, 1979; Virsu and Rovamo, 1979) and temporal frequency (Virsu *et al.*, 1982; Kelly, 1984). There is a debate over vernier acuity (pro scaling: Levi *et al.*, 1985; Virsu *et al.*, 1987; contra evidence: Hering, 1899; Bourdon, 1902; Weymouth, 1958; Westheimer, 1982) and orientation sensitivity (pro: Virsu *et al.*, 1987; contra: Spinelli *et al.*, 1984). The scaling concept fails for two-point separation in the far periphery (Aubert and Foerster, 1857), stereo acuity (Fendick and Westheimer, 1983), scotopic contrast sensitivity (Koenderink *et al.*, 1978b), apparent grating movement (Hilz *et al.*, 1981), numerosity judgement (Parth and Rentschler, 1984), bisection of a straight line (Levi and Klein, 1986; Virsu *et al.*, 1987), positional relations of image components (Rentschler and Treutwein, 1985; Bennett and Banks, 1987; Saarinen, 1987), spatial phase resolution (Harvey *et al.*, 1985) and masking by spatially correlated patterns (Hübner *et al.*, 1985) (for reviews see Weymouth, 1958; Pointer, 1986; Virsu *et al.*, 1987; and Drasdo, 1991).

The relationships between M and retinal eccentricity, proposed by various investigators (Daniel and Whitteridge, 1961; Cowey and Rolls, 1974; Drasdo, 1977, 1989; Rovamo and Virsu, 1979; Schwartz, 1980; Van Essen *et al.*, 1984; Tolhurst and Ling, 1988), are essentially inverse linear functions of the form $M = (1 + aE)^{-1}M_0$, where E is retinal eccentricity in angular degrees from the fovea, and M_0 is the cortical magnification in millimeters per degree at the fovea. The formula is subject to slight modification due to the nonlinearities of $M^{-1}(E)$ found in anatomical (Daniel and Whitteridge, 1961) and electrophysiological (Van Essen *et al.*, 1984) data at larger eccentricities. This correction is achieved by either adding a third-order term in eccentricity E (Rovamo and Virsu, 1979) or by using an exponent of -1.1 in the foregoing equation (Tolhurst and Ling, 1988; Van Essen *et al.*, 1984). The numerical differences between these two formulations are small. Similar

Correspondence to: Hans Strasburger

Received 4 February 1994, revised 29 April 1994, accepted 11 May 1994

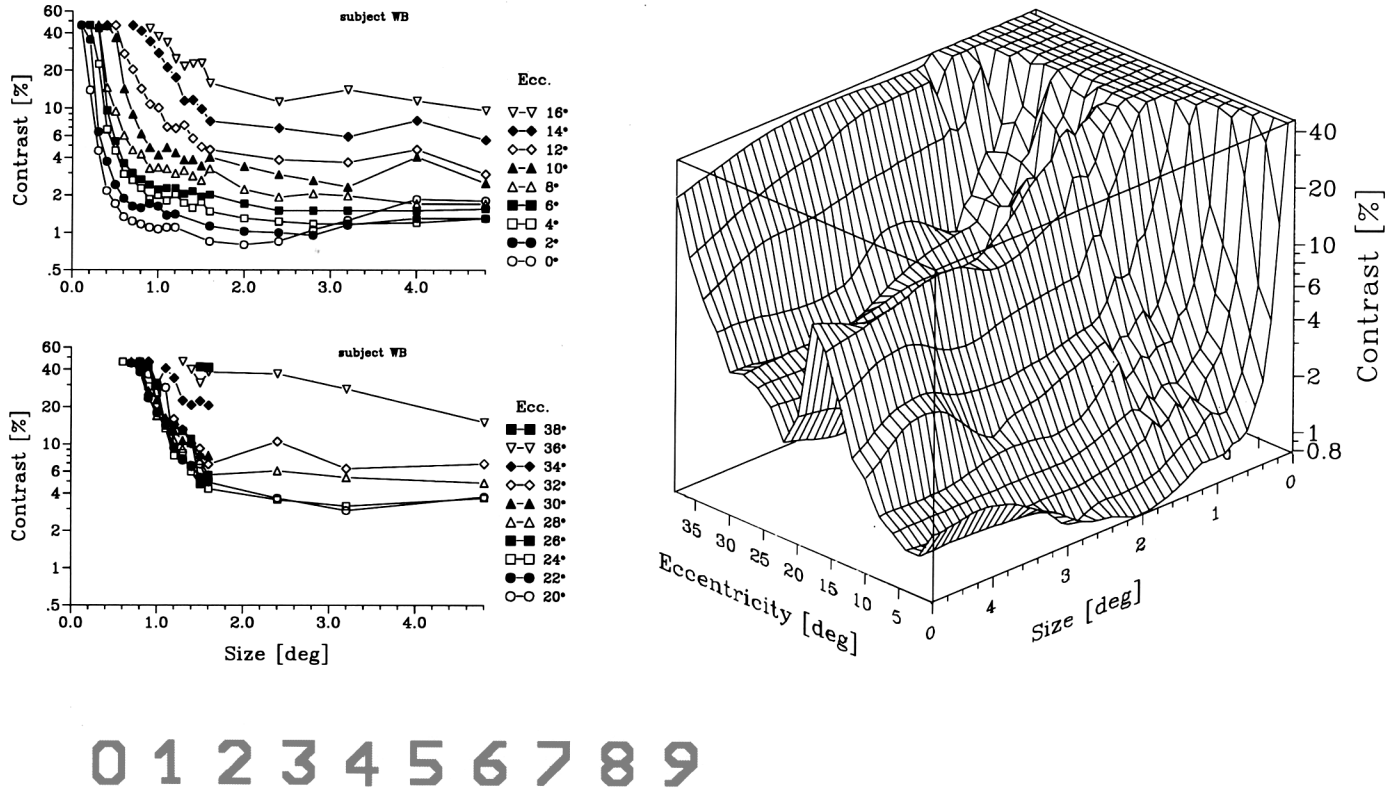

0 1 2 3 4 5 6 7 8 9

FIG. 1. Contrast threshold for recognition of digits (0−9) as a function of angular target size and retinal locus. Since we found no significant differences between thresholds in the left and right visual fields, this figure shows the mean results between the half fields. Contrast thresholds were measured using a computer-controlled maximum-likelihood sequential procedure (Harvey, 1986). This procedure effectively varies the contrast of the target from trial to trial in order to find the contrast giving 67% correct identification. This value represents the point of maximum slope on a Weibull function, which is a good descriptor of the underlying psychometric function. The criterion value is not critical, however, and use of a different value will change the obtained thresholds only slightly. No confusion matrix was recorded. We specify stimulus contrast using the Michelson definition: $(L_{max} - L_{min})/(L_{max} + L_{min})$. The background luminance of the video display was kept constant at 62 cd/m^2. White digits were presented in random order on the video monitor for 100 ms. The experimental setup was identical to that used in a previous study (Strasburger *et al.*, 1991). Subjects fixated a dot located along the horizontal meridian; eccentricity was defined from this point to the target's centre. Viewing was binocular. The 'ridge' in the right figure is in the blind spot (14−18°) where viewing is functionally monocular. Four subjects having normal vision were tested. The largest set of data (~40 000 trials) was obtained from one subject. The main findings were confirmed with three additional subjects. The confidence interval for each data point is 0.13 log units, i.e. the error bars are smaller than the symbols. The inset shows the stimulus character set.

relationships have been reported for retinal ganglion cell density, receptive field centre density and other density measures along the retino-cortical pathway. Since these are of the same functional form as the preceding equation but with different coefficients (Drasdo, 1991), the arguments in the following also apply to these measures.

In the present study we examine the validity of *M*-scaling for the recognition of numerical characters. On the one hand, this classification task is complex since it involves stimulus patterns with an intrinsically 2-D signal variation (see Zetzsche and Barth, 1990). Thus it is impossible to represent the numerals along a single feature dimension such as orientation, length or curvature, and the classification process has to rely on a feature space which has at least two dimensions. On the other hand, numerical character recognition is sufficiently simple in that it resembles the measurement of optotype acuity and involves only one sample for each of the ten signal classes.

As to the psychophysical procedure employed, we measured the threshold contrast that allowed for 67% correct identification of the ten digits 0−9. The stimulus size was kept constant, thus avoiding an interaction between different target sizes and changing scaling factors at different retinal loci. Such measurements were performed for a wide range of target sizes and retinal loci on the horizontal meridian. Viewing was binocular.

Figure 1 shows the recognition performance of one subject, WB (mean of left and right visual fields), as a function of target size and retinal locus. In direct view the lowest contrast thresholds (0.8%) were obtained with digits of 2° size, the thresholds increasing for larger and smaller targets. As target size decreases, contrast thresholds rise steeply until the maximum contrast (46%) possible with our equipment is reached. At high contrast the target size would correspond to conventional visual acuity.

The data for eccentric view are different from those obtained in direct view in two respects: for high contrast conditions the curves are shifted towards larger target sizes. This is in agreement with the idea of cortical magnification scaling. However, the curves are also shifted upwards, to higher contrast values. Size scaling therefore fails to match contrast-versus-size curves from different retinal loci. [Formally, when $C = f_E(S)$ is the relationship between contrast and size at a certain eccentricity, there exists no transformation $g_E(S)$ such that $f_E(S) = f_0(g_E(S))$, simply because the range of function f_E varies with eccentricity E.] To illustrate this failure, we applied *M*-scaling to our data. Figure 2a shows the data which were transformed accordingly for the central 12°. It can be seen how the data points are brought into register at high contrast but not at low contrast values.

This failure of *M*-scaling is further illustrated in Figure 2b, where

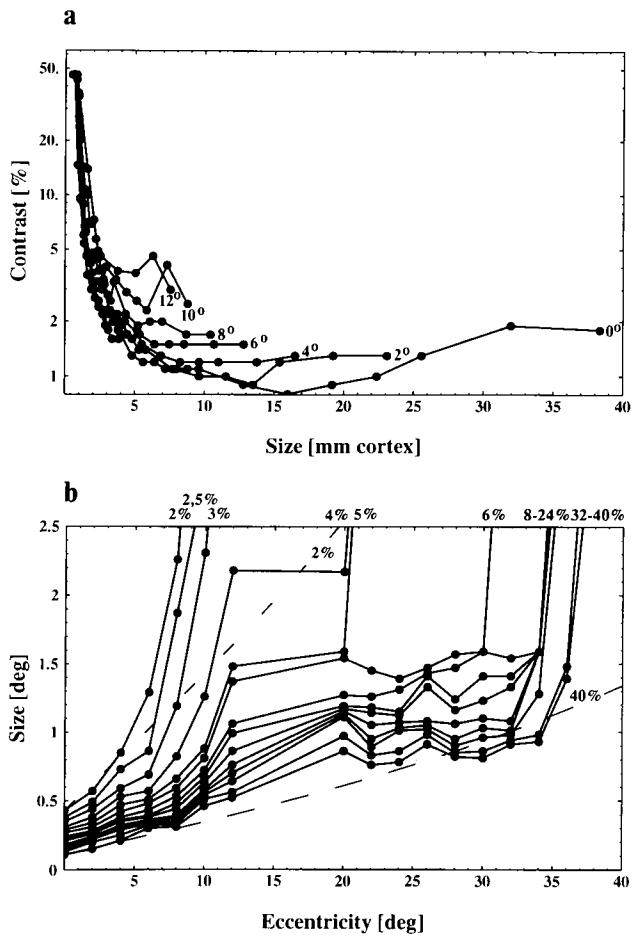

FIG. 2. Failure of M-scaling for the data show in Figure 1. (a) Re-plot of Figure 1 with size M-scaled analogous to Rovamo and Virsu's (1979) figure 4, using their nasal visual field function $M = (1 + 0.33E + 0.00007E^3)^{-1} \cdot M_0$, where E is retinal eccentricity in degrees and M_0 is the magnification in the central fovea, set equal to 7.99 mm of cortex per degree of visual angle. Each stimulus size plotted in this figure was transformed into cortical size by means of $S_c = S_t \cdot M$, where S_t is the target size in degrees of visual angle, S_c is the size of visual cortex onto which the stimulus projects, in millimeters of cortical extent, and M is the nasal magnification factor in mm/° at a given retinal eccentricity from the previous equation. The centre 12° are shown. (b) Threshold target sizes, as a function of retinal eccentricity, for each of a series of threshold contrasts. These target sizes were obtained by interpolation from the data plotted in Figure 1. The dashed lines show predictions from the cortical magnification concept for 2 and 40% contrast. These are obtained by fitting $S = (1 + aE + bE^3) \cdot S_0$ [which follows from the M-scaling equation given in (a) through $S = S_0 \cdot M_0/M$] to the approximately linear portion of our data at a given contrast. In these functions, parameter a determines both the slope, aS_0, and the eccentricity axis intercept, $-1/a$. All curves pass through S_0 on the size axis. Since different estimates of a have been given in the literature, a was treated as a free parameter in the least-squares fit. The amount of curvature, i.e. the ratio b/a, was constrained to be that given in (a) (i.e. 0.00007/0.33), and the curves were constrained to go through S_0 at eccentricity 0. The linear coefficients obtained in these fits were $a = 0.227$ for the 2% curve and $a = 0.209$ for the 40% curve. These coefficients are similar to the value of $a = 0.33$ given by Rovamo and Virsu (1979) [see part (a)].

threshold target sizes are plotted as a function of retinal eccentricity for each of a series of threshold contrasts. At contrasts above, say, 6%, the curves extend far into the periphery in an approximately linear manner. Between ~20 and 30° there is a plateau similar to the one described for the detection of light spots (Harvey and Pöppel, 1972). Further out, target identification becomes difficult or impossible. At low contrasts this behaviour is much more pronounced, leading to an upward curvature at much smaller eccentricities. As a result of this fall-off of performance, the part of the visual field in which recognition is at all possible is sharply reduced. For subject WB it spans no more than 8° at 2% contrast.

Figure 2b also shows predictions based on cortical magnification for 2 and 40% contrast (dashed lines). The slope, a, obtained in both fits is similar to that given by Rovamo and Virsu (1979). At high contrast the function based on cortical magnification fits the data reasonably well up to 34° eccentricity. Although it does not capture the plateau effect between 20 and 30°, it explains 89.7% of the variance out to 34°. Further out, however, it fails to describe the subject's complete inability to identify the target. For lower contrasts the failure of target identification occurs at increasingly less eccentric retinal positions, thus reducing the predictive range of M scaling to a smaller and smaller visual field. This relationship also fails to capture the more pronounced curvatures at lower contrasts.

The scaling transformations considered so far were restricted to the space domain. In the general case, space domain transformations fail to produce invariance of character recognition over the visual field. A parsimonious and complete description of the data can be obtained, however, when scaling is extended to include stimulus contrast. The data in Figure 1, as a function of target size S, essentially follow the geometric locus of a hyperbola, described by the relationship

$$(\log C - \log C_{off}) \cdot (S - S_{off}) = k \qquad (1)$$

with

$$C > C_{off}$$

and

$$S > S_{off}$$

where C_{off} and S_{off} are the asymptotic contrast and size values. They are numerically similar to the minimum contrast and minimum size for each retinal locus and serve to offset the hyperbola away from the origin.

Other non-linear functions could also be fitted; the hyperbola is the simplest of all, though, and its use resulted in excellent fits. Examples of fitting the hyperbolas by means of constrained nonlinear regression are shown in Figure 3a, b. The validity of relationship (1) has been tested by applying it to the mean data of two further subjects (KZ and MB; Strasburger *et al.*, 1991), covering the range 0–12° eccentricity. Using a shape constant of $k = 0.128$, we arrived at a solution that accounted for 98% of the variance.

The offsets C_{off} and S_{off} resulting from these fits show a highly systematic pattern of variation with retinal eccentricity (Fig. 3c and d). The relationship, shown in the figure, can be described by piecewise linear functions:

$$S_{off} = a_1 + a_2E \text{ and } \log C_{off} = a_3 + a_4E \qquad (2)$$

Up to 12° eccentricity, both S_{off} and $\log C_{off}$ vary linearly with eccentricity, at a slope of $a_2 = 0.029$ and $a_4 = 0.058$ respectively. The data fit a straight line especially well, the explained variance being 96.7 and 98.3% respectively. The data of subjects KZ and MB led to similar results (see Table 1). Up to 12°, log contrast offsets and size offsets are also highly correlated to each other ($r = 0.993$).

Between 12 and 30° eccentricity, contrast offsets C_{off} show a plateau, the slope (a_4) dropping to close to zero. For the size offsets S_{off}, the plateau starts beyond the blind spot and extends also up to at least 30° eccentricity (slope $a_2 = -0.0043$). Beyond 30°, contrast offsets increase steeply ($a_4 = 0.097$); size offsets become unreliable, since the

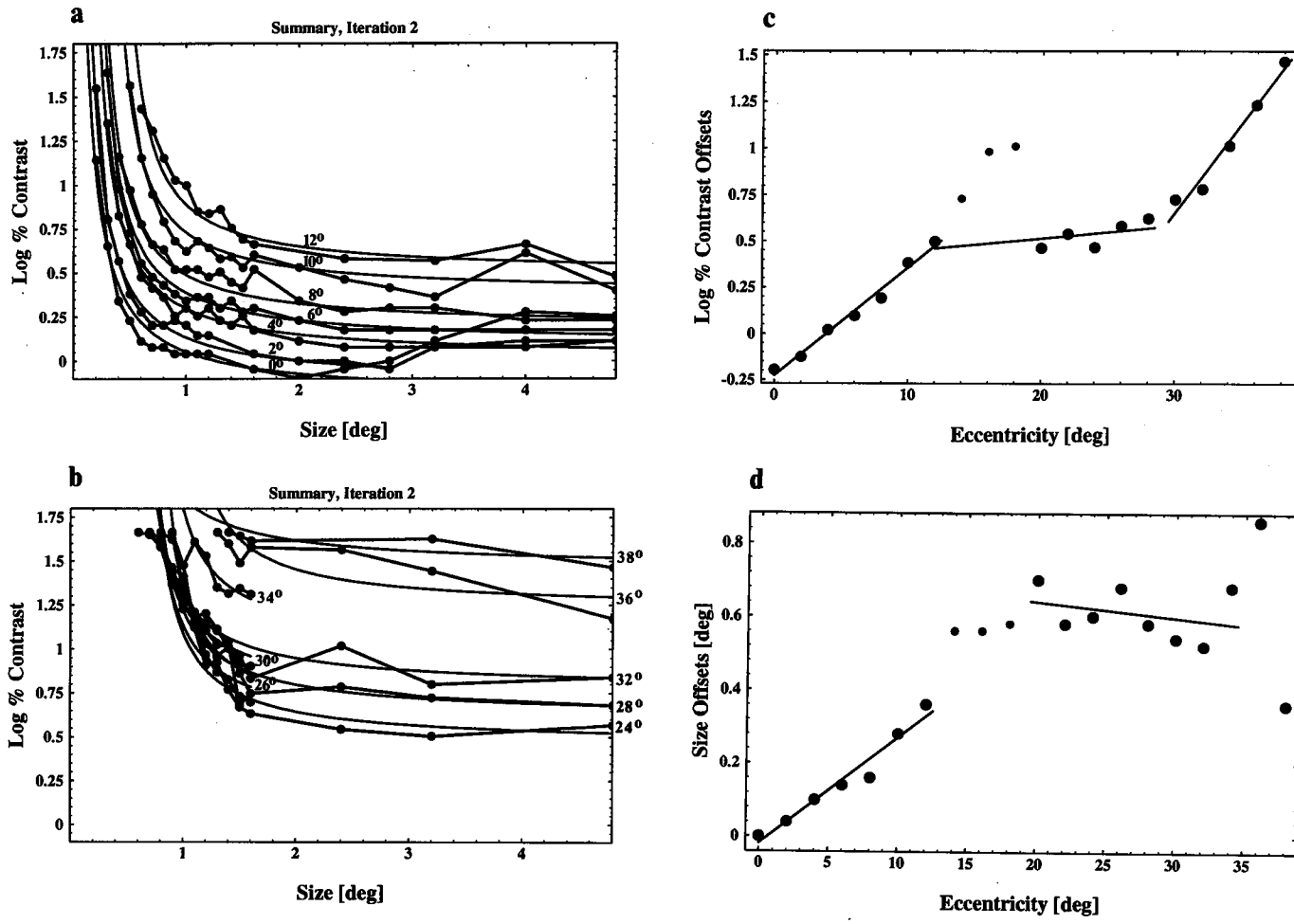

FIG. 3. (a, b) Hyperbolic fits according to equation (1) to data replotted from Figure 1. To fit our data to the hyperbolic function (1), we have performed a constrained nonlinear regression by explicitly minimizing the mean-squared deviation of log contrast. Data obtained in the blind spot were not considered in the fit. Furthermore, the increase in contrast threshold at large target sizes for 0 and 2° eccentricity was excluded and needs to be treated separately. Since equation parameters C_{off}, S_{off} and k are correlated in the regression parameter space, it was necessary to separate the determination of k from that of the offsets C_{off} and S_{off}. The former constant determines the curvature of the hyperbolas. A value of $k = 0.25$ resulted in excellent fits for the three centremost curves (0, 2 and 4°), the explained variance (r^2) being 97.5%. k was then held constant across the retinal locus, while the offsets C_{off} and S_{off} were allowed to vary. The resulting hyperbolas explained 98.4% of the total data variance. (c, d) Contrast and target size offsets resulting from these fits, as a function of retinal eccentricity. Data in the blind spot are shown as smaller points. The relationship shown in (d) can serve as a psychophysical estimate of the anatomical magnification factor M.

TABLE 1. Parameters for a full description of our data set (equations 1 and 2)

Retinal eccentricity		0−12°	14−18°	20−30°	30−40°
sj. WB	a_1	−0.02	−0.02	0.73	–
	a_2	0.029	0.029	−0.0043	–
	a_3	−0.23	0.38	0.38	−2.25
	a_4	0.058	0.0068	0.0068	0.097
	k	–	0.25	–	–
sj. KZ/MB	a_1	constr. to 0			
	a_2	0.033			
	a_3	constr. to 0			
	a_4	0.075			
	k	0.128			

contrast thresholds are close to the maximum contrasts in our setup. These parameters are summarized in Table 1.

Equations (1) and (2) together fully describe our data. They can be combined to derive a functional relationship, like that shown in Figure 2b, between target size S and eccentricity, as a generalization of the M-scaling equation. It differs from the standard form in that it contains a nonlinear term, the contribution of which is negligible at high contrast but at low contrast goes to infinity at a certain eccentricity.

The size offsets S_{off} at various eccentricities obtained in the fit (equation 2a) can be considered to provide a direct description of the changes of spatial scale across the retina. The functional relationship depicted in Figure 3d thus gives a psychophysical estimate of the anatomical magnification factor M. Except for the plateau effect, it is in rough correspondence with the anatomical data.

We have thus found variations in character recognition across the visual field which are incompatible with the (scalar) cortical magnification concept. This incompatibility is a consequence of the limited extent to which recognition contrast sensitivity can be improved by increasing target size and is not a matter of what the precise relationship between cortical magnification and retinal position is. Explanations based on the topological mapping can therefore not account for our results. This includes differences in the M factor between different cell types, e.g. between parvo and magno cells [compare Drasdo's (1989) fig. 2 with the present Fig. 2b], and other explanations based on the spatial mapping from retina to cortex, including nonconformal maps (Mallot *et al.*, 1990).

With optimal size scaling applied, recognition contrast thresholds still increase ~10-fold between the fovea and 32° eccentricity. The question arises whether such a variation can be due to the properties of the retino-cortical pathway. For an answer, three properties of this pathway need be considered: variations in contrast sensitivity of ganglion cells, variations in the receptive field overlap factor or sampling density, and variations in positional uncertainty.

With regard to the first property, cells from the magnocellular pathway (M cells) have higher contrast sensitivity than parvo (P) cells (Derrington and Lennie, 1984; Hicks *et al.*, 1983), the optimum M cell contrast threshold being 1% whereas P cells reach only ~10% contrast. It thus seems likely that the optimum contrast threshold for character recognition is mediated by M cells. Although M cells have an [8-fold lower sampling density than P cells (Perry *et al.*, 1984; Kaplan *et al.*, 1990), it is sufficient to mediate optimum contrast thresholds at all retinal positions since these thresholds always go together with relatively large target sizes. The variation of the contrast sensitivity of primate M cells over the visual field is not documented by Hicks *et al.* (1983) or Derrington and Lennie (1984) but the overall similarity of primate M cells to cat X and Y ganglion cells (Kaplan *et al.*, 1990) makes it likely that Fischer and May's (1970) result obtained in the cat also holds for the present case. These authors have shown that the contrast sensitivity of ganglion cells for small dots decreases with retinal eccentricity in inverse proportion to a simultaneous increase in receptive field size. Thus, for appropriately scaled stimuli the detection contrast sensitivity of ganglion cells becomes independent of retinal position. Current models of visual processing are based on this premiss (Mallot *et al.*, 1990; Bijl *et al.*, 1992). It also corresponds reasonably well to psychophysical findings concerning grating detection (Koenderink *et al.*, 1978b; Virsu and Rovamo, 1979), where contrast sensitivity, after appropriate size scaling, varies by a factor of ~2. However, detection presumably depends on the most sensitive cells whereas recognition requires some kind of feature combination and may therefore be limited by the least sensitive contributing cells. All available evidence thus points to the conclusion that contrast sensitivity of ganglion cells is not the basis of peripheral recognition contrast thresholds.

The second property of the retino-cortical pathway that needs to be considered is the varying sampling density or the overlap factor of receptive fields, i.e. the number of ganglion cells covering a point in visual space. This factor is incorporated in two recent models, one by Bijl *et al.* (1992), designed to describe the detection of Gaussian blobs, and one by Wilson (1991), designed to describe hyperacuity and masking. Bijl *et al.* (1992) assume a reduction in detection sensitivity proportional to the square root of the overlap factor. However, this leads to the prediction of a decrease in sensitivity for grating detection which only amounts to a factor of three between the fovea and 42° eccentricity, i.e. much less than we find for character recognition. The response pooling attained by the receptive field overlap would also be more effective for detection (since in that case there are more features to pool) than for recognition, so that, on the basis of overlap, one would predict an even lower peripheral sensitivity reduction in recognition.

The third possibility, the assumption of a varying precision of the spatial position code, is part of Wilson's (1991) model and leads to an improved prediction of hyperacuity behaviour there. It cannot account for the decrease in optimum recognition contrast threshold that we found since it concerns the mapping: sufficient enlargement of the stimuli at a fixed position will reduce the influence of positional jitter, thereby removing any reduction in contrast sensitivity introduced by the latter.

To summarize, recognition of high contrast characters is, on the one hand, captured by cortical magnification, whereas recognition of low contrast characters is not. On the other hand, detection tasks generally seem to obey M-scaling or some other kind of spatial scaling law. From the latter observation we conclude that detection thresholds arise in the retino-cortical pathway and are fully determined by its sampling characteristics. Unlike detection performance, pattern recognition critically depends, at least in the case of intrinsically >1-D stimuli, on the combination of several feature dimensions (Watanabe, 1985). The neural process of combination must be expected to introduce its own set of thresholds in the sense that the feature weights must be large enough along all relevant perceptual dimensions in order to preserve the full amount of information necessary for the subsequent recognition process. Clearly, these 'combination thresholds'exist on top of those of the retino-cortical pathway and we interpret the observed recognition thresholds as their behavioural correlate. Furthermore, our results imply that these combination thresholds arise not in the retino-cortical pathway but in the primary visual cortex itself or at a functionally later stage. This view is supported by recent clinical and neurophysiological evidence. From observations with patients suffering from visual agnosia and from single-unit responses to illusory contours, Baumgartner (1990) has contended that cortical area V1 is 'a detecting but not a perceiving device' and that 'object perception begins not before V2'. Fujita *et al.* (1992) showed that low-level features are combined in post-V1 areas to subserve the task of recognition. Thus we conclude that the conventional scalar cortical magnification theory fails for recognition tasks since they involve the processing properties of striate and prestriate areas which cannot be captured by a single scaling factor (see Livingstone and Hubel, 1985; Rentschler and Treutwein, 1985; Bennett and Banks, 1987).

Acknowledgements

We thank Alan Cowey and Heinz Wässle for helpful comments on the manuscript. The study was supported by grants Re 337/5 and Po 121/13 (Proj. 5 to I. R.) of the Deutsche Forschungsgemeinschaft.

Abbreviations

M cells	cells from the magnocellular pathway
P cells	parvo cells

References

Aubert, H. and Foerster, O. (1857) Beiträge zur Kenntniss des indirecten Sehens. (I). Untersuchungen über den Raumsinn der Retina. *Arch. Ophthalmol.*, **3**, 1–37.

Baumgartner, G. (ed.). (1990) *Where do Visual Signals Become a Perception?* Pontificia Academia Scientiarum, Civitas Vaticana.

Bennett, P. J. and Banks, M. S. (1987) Sensitivity loss in odd-symmetric mechanisms and phase anomalies in peripheral vision. *Nature*, **326**, 873–876.

Bijl, P., Koenderink, J. J. and Kappers, A. M. L. (1992) Deviations from strict M scaling. *J. Opt. Soc. Am.*, **9**, 1233–1239.

Bourdon, B. (1902) *La Perception Visuelle de l'Espace*. Schleicher, Paris.

Cowey, A. and Rolls, E. T. (1974) Human cortical magnification factor and its relation to visual acuity. *Exp. Brain Res.*, **21**, 447–454.

Daniel, P. M. and Whitteridge, D. (1961) The representation of the visual field on the cerebral cortex in monkeys. *J. Physiol.*, **159**, 203–221.

Derrington, A. M. and Lennie, P. (1984) Spatial and temporal contrast sensitivities of neurones in lateral geniculate nucleus of macaque. *J. Physiol.*, **357**, 219–240.

Drasdo, N. (1977) The neural representation of visual space. *Nature*, **266**, 554–556.

Drasdo, N. (1989) Receptive field densities of the ganglion cells of the human retina. *Vision Res.*, **29**, 985–988.

Drasdo, N. (1991) Neural substrates and threshold gradients of peripheral vision. In Kulikowski, J. J. (ed.), *Limits of Vision*. Macmillan, London, pp. 250–264.

Fendick, M. and Westheimer, G. (1983) Effects of practice and the separation of test targets on foveal and peripheral stereoacuity. *Vision Res.*, **23**, 145–150.

Fischer, B. and May, H. U. (1970) Invarianzen in der Katzenretina: Gesetzmässige Beziehungen zwischen Empfindlichkeit, Grösse und Lage receptiver Felder von Ganglienzellen. *Exp. Brain Res.*, **11**, 448–464.

Fujita, I., Tanaka, K., Ito, M. and Cheng, K. (1992) Columns for visual features of objects in monkey inferotemporal cortex. *Nature*, **360**, 343–346.

Harvey, L. O., Jr (1986) Efficient estimation of sensory thresholds. *Behav. Res. Methods Instrum. Comput.*, **18**, 623–632.

Harvey, L. O., Jr and Pöppel, E. (1972) Contrast sensitivity of the human retina. *Am. J. Opt. Arch. Am. Acad. Opt.*, **49**, 748–753.

Harvey, L. O., Jr, Rentschler, I. and Weiss, C. (1985) Sensitivity to phase distortion in central and peripheral vision. *Percept. Psychophys.*, **38**, 392–396.

Hering, E. (1899) Über die Grenzen der Sehschärfe. *Ber. Verhand. Königlich-Sächsischen Gesell. Wissensch. Leipzig/Math.-Phys. Classe: Naturwissenschaft. Teil*, 16–24.

Hicks, T. P., Lee, B. B. and Vidyasagar, T. R. (1983) The responses of cells in macaque lateral geniculate nucleus to sinusoidal gratings. *J. Physiol.*, **337**, 183–200.

Hilz, R. and Cavonius, C. R. (1974) Functional organization of the peripheral retina: Sensitivity to periodic stimuli. *Vision Res.*, **14**, 1333–1337.

Hilz, R., Rentschler, I. and Brettel, H. (1981) Insensitivity of peripheral vision to spatial phase. *Exp. Brain Res.*, **43**, 111–114.

Hübner, M., Rentschler, I. and Encke, W. (1985) Hidden-face recognition: Comparing foveal and extrafoveal performance. *Hum. Neurobiol.*, **4**, 1–7.

Kaplan, E., Lee, B. B. and Shapley, R. M. (1990) Chapter 7. New views of primate retinal function. *Prog. Retinal Res.*, **9**, 273–336.

Kelly, D. H. (1984) Retinal inhomogeneity: I. Spatiotemporal contrast sensitivity. *J. Opt. Soc. Am. A*, **1**, 107–113.

Koenderink, J. J., Bouman, M. A., Bueno de Mesquita, A. E. and Slappendel, S. (1978a) Perimetry of contrast detection thresholds of moving spatial sine wave patterns. III. The target extent as a sensitivity controlling parameter. *J. Opt. Soc. Am.*, **68**, 854–860.

Koenderink, J. J., Bouman, M. A., Bueno de Mesquita, A. E. and Slappendel, S. (1978b) Perimetry of contrast detection thresholds of moving spatial sinewave patterns. IV. The influence of the mean retinal illuminance. *J. Opt. Soc. Am.*, **68**, 860–865.

Levi, D. M. and Klein, S. A. (1986) Sampling in spatial vision. *Nature*, **320**, 360–362.

Levi, D. M., Klein, S. A. and Aitsebaomo, A. P. (1985) Vernier acuity, crowding and cortical magnification. *Vision Res.*, **25**, 963–977.

Livingstone, M. S. and Hubel, D. H. (1985) Spatial relationship and extrafoveal vision. *Nature*, **315**, 285.

Ludvigh, E. (1941) Extrafoveal visual acuity as measured with Snellen test letters. *Am. J. Ophthalmol.*, **24**, 303–310.

Mallot, H. A., von Seelen, W. and Giannakopoulos, F. (1990) Neural mapping and space-variant image processing. *Neural Networks*, **3**, 245–263.

Ogle, K. N. (1950) *Researches in Binocular Vision*. W. B. Saunders, Philadelphia, PA.

Parth, P. and Rentschler, I. (1984) Numerosity judgements in peripheral vision: limitations of the cortical magnification hypothesis. *Behav. Brain Res.*, **11**, 241–248.

Perry, V. H. and Cowey, A. (1985) The ganglion cell and cone distributions in the monkey's retina: implications for central magnification factors. *Vision Res.*, **12**, 1795–1810.

Perry, V. H., Oehler, R. and Cowey, A. (1984) Retinal ganglion cells that project to the dorsal lateral geniculate nucleus in the macaque monkey. *Neuroscience*, **12**, 1101–1123.

Pointer, J. S. (1986) The cortical magnification factor and photopic vision. *Biol. Rev. Camb. Phil. Soc.*, **61**, 97–119.

Rentschler, I. and Treutwein, B. (1985) Loss of spatial phase relationships in extrafoveal vision. *Nature*, **313**, 308–310.

Rovamo, J. and Virsu, V. (1979) An estimation and application of the human cortical magnification factor. *Exp. Brain Res.*, **37**, 1–20.

Rovamo, J., Virsu, V. and Näsänen, R. (1978) Cortical magnification factor predicts the photopic contrast sensitivity across the visual field. *Nature*, **271**, 54–56.

Saarinen, J. (1987) Perception of positional relationships between line segments in eccentric vision. *Perception*, **16**, 583–591.

Schwartz, E. L. (1980) Computational anatomy and functional architecture of striate cortex: a spatial mapping approach to perceptual coding. *Vision Res.*, **20**, 645–669.

Spinelli, D., Bazzeo, A. and Vicario, G. B. (1984) Orientation sensitivity in the peripheral visual field. *Perception*, **13**, 41–47.

Strasburger, H., Harvey, L. O., Jr and Rentschler, I. (1991) Contrast thresholds for identification of numeric characters in direct and eccentric view. *Percept. Psychophys.*, **49**, 495–508.

Tolhurst, D. J. and Ling, L. (1988) Magnification factors and the organization of the human striate cortex. *Hum. Neurobiol.*, **6**, 247–254.

Van Essen, D. C., Newsome, W. T. and Maunsell, H. R. (1984) The visual field representation in striate cortex of the macaque monkey: asymmetries, anisotropies and individual variability. *Vision Res.*, **24**, 429–448.

Virsu, V. and Rovamo, J. (1979) Visual resolution, contrast sensitivity and cortical magnification factor. *Exp. Brain Res.*, **37**, 475–494.

Virsu, V., Rovamo, J., Laurinen, P. and Näsänen, R. (1982) Temporal contrast sensitivity and cortical magnification. *Vision Res.*, **22**, 1211–1217.

Virsu, V., Näsänen, R. and Osmoviita, K. (1987) Cortical magnification and peripheral vision. *J. Opt. Soc. Am. A*, **4**, 1568–1578.

Wässle, H., Grünert, U., Röhrenbeck, J. and Boycott, B. B. (1989) Cortical magnification factor and the ganglion cell density of the primate retina. *Nature*, **341**, 643–646.

Watanabe, S. (1985) *Pattern Recognition: Human and Mechanical*. John Wiley, New York.

Wertheim, T. (1894) Über die indirekte Sehschärfe. *Zeitschr. Psychol. Physiol. Sinnesorg.*, **7**, 172–187.

Westheimer, G. (1982) The spatial grain of the perifoveal visual field. *Vision Res.*, **22**, 157–162.

Weymouth, F. W. (1958) Visual sensory units and the minimal angle of resolution. *Am. J. Ophthalmol.*, **46**, 102–113.

Wilson, H. R. (1991) Model of peripheral and amblyopic hyperacuity. *Vision Res.*, **31**, 967–982.

Zetzsche, C. and Barth, E. (1990) Fundamental limits of linear filters in the visual processing of two-dimensional signals. *Vision Res.*, **30**, 1111–1117.